Revealing Real-Time Emotional Responses: a Personalized Assessment based on Heartbeat Dynamics

Gaetano Valenza[1,2,3], Luca Citi[1,2,4], Antonio Lanatá[3],
Enzo Pasquale Scilingo[3], Riccardo Barbieri[1,2]

1. Neuroscience Statistics Research Laboratory, Massachusetts General Hospital, Harvard Medical School, Boston, MA, 02114, USA

2. Department of Brain and Cognitive Sciences, Massachusetts Institute of Technology, Cambridge, MA 02139, USA

3. Department of Information Engineering and Research Centre E Piaggio, University of Pisa, Pisa, Italy

4. School of Computer Science and Electronic Engineering, University of Essex, Colchester, CO43SQ, UK

September 25, 2013

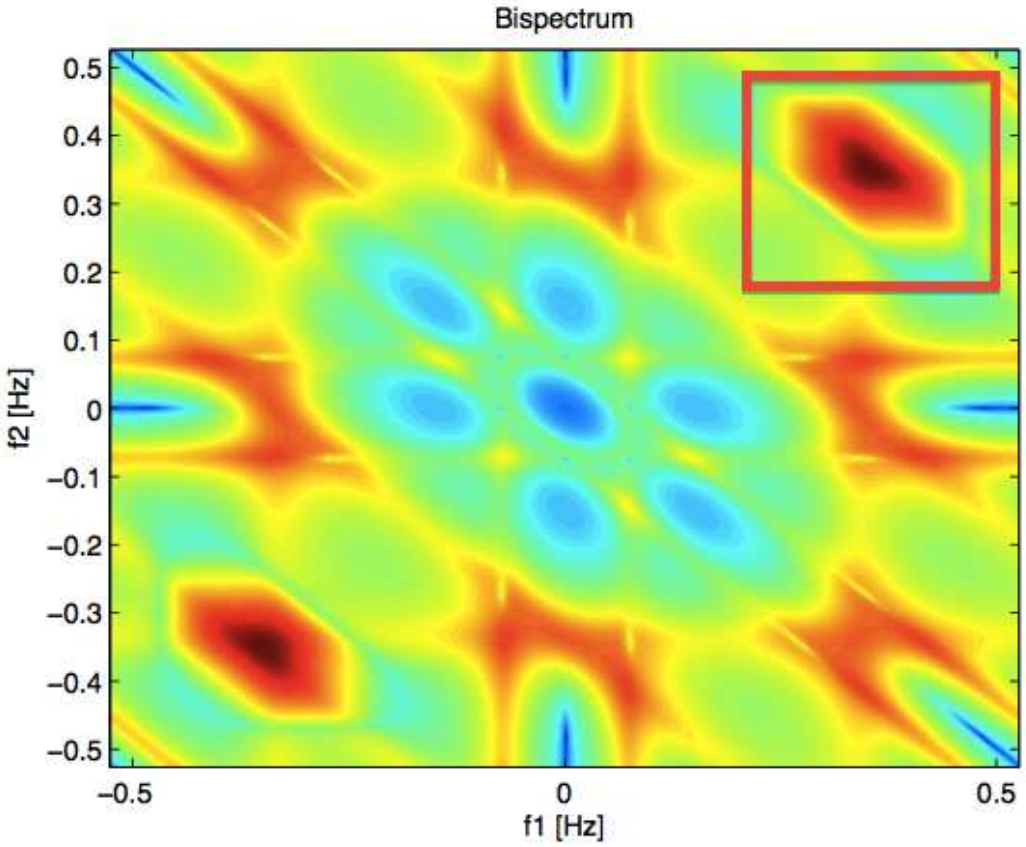

Figure 1: An explanatory example of bispectral plane during parasympathetic dominance. The bispectrum has been estimated using the instantaneous NARI point-process based analysis on RR interval series acquired during supine rest condition. The red square indicates the region of highest power on the high-frequency band for each axis.

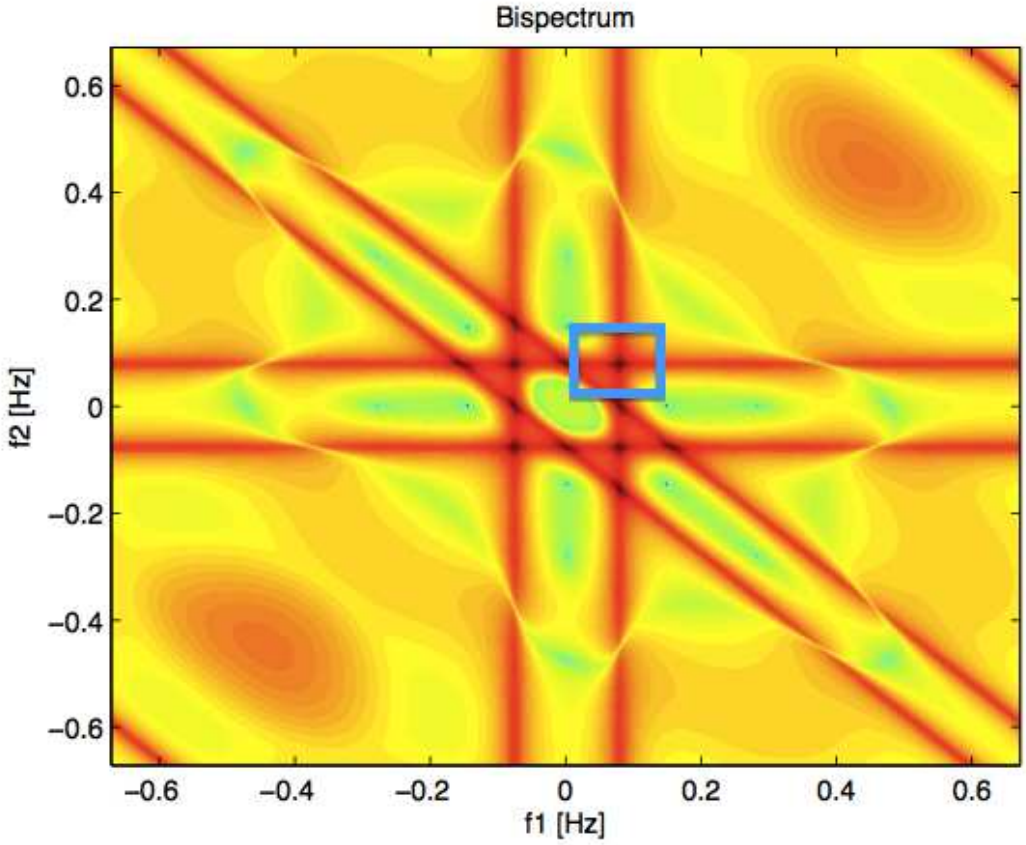

Figure 2: An explanatory example of bispectral plane during sympathetic dominance. The bispectrum has been estimated using the instantaneous NARI point-process based analysis on RR interval series acquired after postural changes by means of tilt table. The red square indicates the region of highest power on the low-frequency band for each axis.

Table 1: Instantaneous bispectral features from the point-process NARI model

Feature Name	Parameters	Math. Derivation	Formula
Bispectral Invariants [1]	$0 < a \leq 1$ $j = \sqrt{-1}$	$I(a,t) = I_r(a,t) + jI_i(a,t) = \int_{f_1=0^+}^{\frac{1}{1+a}} \mathrm{Bis}(f_1, af_1, t) df_1$ $P(a,t) = \arctan\left(\frac{I_i(a,t)}{I_r(a,t)}\right)$	$\overline{P(a,t)}$ $\sigma_{P(a,t)}$
Mean Magnitude [2]	-	-	$M_{\mathrm{mean}}(t) = \frac{1}{L}\sum_\Omega \lvert\mathrm{Bis}(f_1, f_2, t)\rvert$
Phase Entropy [2]	$n = 0, 1, \ldots N-1$	$p(\Psi_n, t) = \frac{1}{L}\sum_\Omega 1\left(\Phi\left(\mathrm{Bis}(f_1, f_2, t)\right)\right) \epsilon \Psi_n$ $\Psi_n = \{\Phi \lvert -\pi + 2\pi n/N \leq \phi \leq -\pi + 2\pi(n+1)/N\}$	$P_e(t) = \sum_n p(\Psi_n, t)\log(p(\Psi_n, t))$
Normalized Bispectral entropy [3]	-	$p_n(t) = \frac{\lvert\mathrm{Bis}(f_1,f_2,t)\rvert}{\sum_\Omega \lvert\mathrm{Bis}(f_1,f_2,t)\rvert}$	$P_1(t) = -\sum_n p_n(t)\log(p_n(t))$
Normalized Bispectral squared entropy [3]	-	$p_n(t) = \frac{\lvert\mathrm{Bis}(f_1,f_2,t))\rvert^2}{\sum_\Omega \lvert\mathrm{Bis}(f_1,f_2,t)\rvert^2}$	$P_2(t) = -\sum_n p_n(t)\log(p_n(t))$
Sum of Logarithmic Bispectral Amplitudes [4]	-	-	$\mathrm{Hbis}_1(t) = \sum_\Omega \log\left(\lvert\mathrm{Bis}(f_1, f_2, t)\rvert\right)$
Nonlinear Sympatho-Vagal Interactions	-	-	$\mathrm{LL}(t) = \int_{f_1=0^+}^{0.15}\int_{f_2=0^+}^{0.15} \mathrm{Bis}(f_1, f_2, t) df_1 df_2$ $\mathrm{LH}(t) = \int_{f_1=0^+}^{0.15}\int_{f_2=0.15^+}^{0.4} \mathrm{Bis}(f_1, f_2, t) df_1 df_2$ $\mathrm{HH}(t) = \int_{f_1=0.15^+}^{0.4}\int_{f_2=0.15^+}^{0.4} \mathrm{Bis}(f_1, f_2, t) df_1 df_2$

Table 2: Experimental results on the Autocorrelation plot statistics using point-process linear and NARI models. Columns refer to: subject identifier, number of points outside the confidence interval (CI), Sum of the Squared Distances (SSD) of the points outside the CI. For each subject, *linear* stands for values given by the linear point-process model, whereas *nonlinear* stands for values given by NARI models. The tick indicates improvements (i.e., reductions of the number of points outside the CI or SSD) given by the use of NARI models.

	Number of Points outside CI		SSD	
Subjects	Linear→Nonlinear		Linear→Nonlinear	
1	10→6	√	0.3103→0.0718	√
2	15→4	√	0.2166→0.0722	√
3	12→1	√	0.2576→0.0001	√
4	10→4	√	0.1842→0.0656	√
5	11→5	√	0.1327→0.0437	√
6	4→1	√	0.1031→0.0124	√
7	3→2	√	0.0925→0.0229	√
8	11→2	√	0.2511→0.0280	√
9	9→6	√	0.1661→0.0701	√
10	6→6		0.1220→0.0338	√
11	10→6	√	0.1028→0.0457	√
12	11→3	√	0.2058→0.0143	√
13	9→8	√	0.1205→0.0501	√
14	7→2	√	0.2529→0.0160	√
15	8→3	√	0.1242→0.0219	√
16	15→9	√	0.1998→0.0660	√
17	10→1	√	0.2597→0.0001	√
18	10→5	√	0.2492→0.0549	√
19	7→4	√	0.1188→0.0243	√
20	11→3	√	0.1529→0.0436	√
21	11→3	√	0.1513→0.0501	√
22	12→2	√	0.2095→0.0126	√
23	15→5	√	0.3251→0.0718	√
24	5→3	√	0.0904→0.0165	√
25	6→6		0.0933→0.0509	√
26	7→1	√	0.1068→0.0185	√
27	6→5	√	0.0675→0.0408	√
28	6→4	√	0.0903→0.0470	√
29	10→2	√	0.2272→0.0172	√
30	8→2	√	0.1779→0.0136	√

References

[1] V. Chandran and S. Elgar, Pattern recognition using invariants defined from higher order spectra-one dimensional inputs, Signal Processing, IEEE Transactions on, 41, 1, 205 (1993).

[2] T. Ng, S. Chang, and Q. Sun, Blind detection of photomontage using higher order statistics, in Circuits and Systems, 2004. ISCAS'04. Proceedings of the 2004 International Symposium on, 5 IEEE,V–688 (2004).

[3] K. Chua, V. Chandran, U. Acharya, and C. Lim, Application of higher order statistics/spectra in biomedical signals–a review, Medical engineering & physics, 32, 7, 679–689 (2010).

[4] S. Zhou, J. Gan, and F. Sepulveda, Classifying mental tasks based on features of higher-order statistics from eeg signals in brain-computer interface, Information Sciences, 178, 6, 1629–1640 (2008).